

## **A REVIEW OF FAILURE MODES OF NUCLEAR FUEL CLADDING**

M. A. KHATTAK<sup>1,\*</sup>, ABDOULHDI A. BORHANA OMRAN<sup>2</sup>, S. KAZI<sup>3</sup>,  
M. S. KHAN<sup>4</sup>, HAFIZ M. ALI<sup>5</sup>, SYEDA L. TARIQ<sup>6</sup>, MUHAMMAD A. AKRAM<sup>7</sup>

<sup>1</sup>ARL Laboratory Services PTY Ltd. Yennora, Sydney NSW 2161, Australia

<sup>2</sup>Department of Mechanical Engineering, Universiti Tenaga Nasional, Selangor, Malaysia

<sup>3</sup>Faculty of Engineering Science and Technology, Isra University, Hyderabad, Sindh-Pakistan

<sup>4</sup>School of Mechanical and Manufacturing Engineering, NUST, Islamabad, Pakistan

<sup>5,6,7</sup>Mechanical Engineering Department, University of Engineering and Technology  
Taxila, Pakistan

\*Corresponding Author: adil@arllabservices.com.au

### **Abstract**

In this research, an effort has been made to systematically establish the research studies managed on assortment of nuclear fuel cladding materials since the initial reactors, revealing some of the main failure modes and briefly reflecting the challenges facing the progress of fuel cladding materials and clad tube failure for future generation of reactors. An introduction to various clad materials has been added, in which the result of alloying elements on the material properties have been presented. Each subsection of the review has been provided with some tables and figures. The small part on determining a good fuel clad has also been encompassed. The last section of the review has been devoted to accidents occur related to fuel clad. About 101 published studies (1965-2017) are examined in this review. It is noticeable from the review of articles that increase in corrosion and creep rate during Loss of Coolant Accident (LOCA) are significant. During corrosion, oxide layers formed on the clad surface are brittle which would endanger the structural integrity. Creep deformation cause cladding tube ballooning.

Keywords: Criteria, Failure, Fuel cladding, Nuclear reactor, Zirconium alloy.

### 1. Introduction

As a result of the great earthquake of east Japan, along with the catastrophic tsunami, the Fukushima Daiichi BWR plants were severely damaged. The nuclear regulatory body in Japan Nuclear and Industrial Safety Agency (NISA), acknowledged the Fukushima nuclear accident was at the Level five on INES (International Nuclear and Radiological Event Scale)-the same level of the nuclear accident at Three Mile Island in 1979. NISA re-evaluated the level of accident to the maximum level of seven on INES on April 12, putting it on a par with the Chernobyl accident in 1986 [1-3]. This fission product restraint capability of the cladding was lost in both accidents because zircaloy reacted with water releasing large quantities of flammable hydrogen gas, zircaloy reacted exothermically with water during the accident releasing a large amount of heat and zircaloy lost all of its strength upon heating above 500°C and ballooned, blocking flow to the core interior [4, 5]. These events generated serious discussion in the United States to develop fuel and cladding improvements that would be more accident tolerant and give operators more time to employ mitigation measures during accidents to minimize core degradation, fuel failure and fission product release. The nuclear power plant was built with different material and design to operate in safe condition [6].

Nuclear reactors initially served as in three general purposes, which are civilian reactor, military reactor and research reactor. Civilian reactor is used to generate energy for electricity, military reactor is used to create Plutonium-239 for nuclear weapons and research reactor is used for training purposes, production of isotopes for medicine and nuclear physics experimentation, moreover, there are 5 types of generations which are Generation I, II, III, III+ and IV [7, 8]. Comparison between types of nuclear reactor in Generation II is shown in Table 1.

**Table 1. Comparison between types of nuclear reactor in Generation II.**

<b>Types of reactor</b>	Pressurized Water Reactor (PWR)	Boiling Water Reactor (BWR)	Canada Deuterium Uranium Reactor (CANDU)	Advanced Gas-cooled Reactor (AGR)	Vodoyanoi Energeticheskiye Reactory (VVER)
<b>Purpose</b>	Electricity [9]	Electricity, nuclear powered ships (U.S [9])	Electricity [10]	Electricity, plutonium production [9]	Electricity [11]
<b>Coolant Type</b>	Light water (H <sub>2</sub> O) [9]	Light water (H <sub>2</sub> O) [9]	Heavy water (D <sub>2</sub> O) [10]	Gas (carbon dioxide or helium) [9]	Light water (H <sub>2</sub> O) [11]
<b>Moderator Type</b>	Light water (H <sub>2</sub> O) [9]	Light water (H <sub>2</sub> O) [9]	Heavy water (D <sub>2</sub> O) [10]	Graphite [9]	Light water (H <sub>2</sub> O) [11]
<b>Fuel-Chemical</b>	Uranium dioxide	Uranium dioxide (UO <sub>2</sub> ) [9]	Uranium dioxide (UO <sub>2</sub> ) [10]	Uranium dicarbide (UC <sub>2</sub> ) or uranium metal [9]	Uranium dioxide (UO <sub>2</sub> ) [11]

<b>Composition</b>	(UO <sub>2</sub> ) [9]				
<b>Fuel-Enrichment Level</b>	Low-enriched [9]	Low-enriched [9]	Slightly enriched uranium, [10]	Slightly-enriched, natural uranium [9]	2.3%, 3.3% and 4.4% enrichment fuel [11]
<b>Fuel Cladding material</b>	Zircaloy-4 and Zircaloy-2 [10]	Zircaloy-2 [9]	Zircaloy-2 and zircaloy-4 [10]	Stainless steel [12]	E110 (Zr1wt.%Nb) [11]

The design limitation encompasses the neutron absorption, the creep resistance, the neutron radiation endurance and the maximum service temperature[13-17].

Many multi-component systems, which incorporate metallic and ceramic systems, might be contemplated as potential novel materials for nuclear fuel cladding in terms of neutron economy [15, 16].

Correlation between neutron absorption cross-section for unpolluted elements versus temperature resistance is shown in Fig. 1 [18]. The radiation resistant should also be considered in choosing fuel cladding material. As a consequence, it will alter the properties of the material, providing the temperature is lower than 40% of the temperature [19].Conclusively, the cladding material needed to be corrosion resistant to the environment [20, 21].

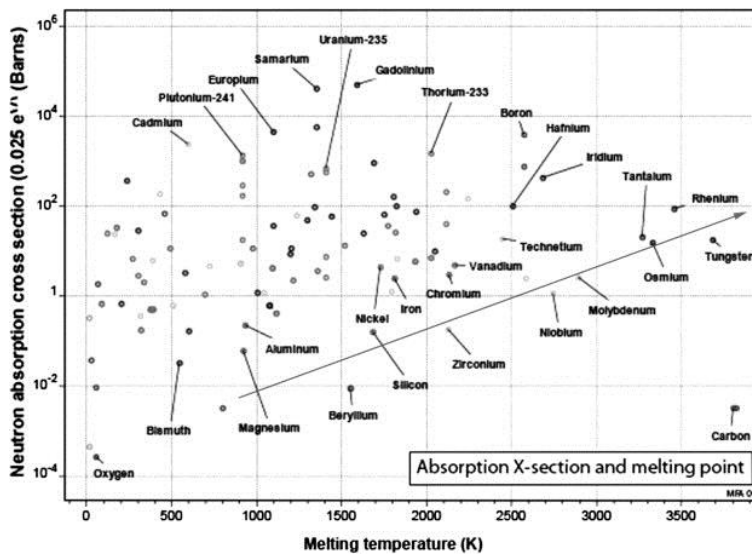


**Fig. 1. Neutron absorption cross-section for unpolluted elements versus temperature resistance [18].**

Several accidents related to the failure of the cladding are reported by Tanveer Alam et al. [22]. The most common accident related to the failure of the cladding material is Grid to rod fretting, Debris fretting, Corrosion, Pellet-clad interaction, Manufacturing defects, and Cladding collapse. Grid to rod fretting is one of the major failures for PWR [21].

## 2. Fuel Cladding Material Selection

Design limitations of cladding comprises the neutron absorption cross section, the maximum service temperature, the creep resistance, the mechanical strength, the toughness, the neutron radiation resistance and the thermal expansion [13-18]. Material with worthy neutron economy is a probable cladding material. Due to this purpose, numerous multi-component systems merging Be, C, Mg, Zr, Si, and O might be studied as potential new materials for nuclear fuel cladding. In fact, Al, Mg, and Zr alloys have formerly been used as fuel cladding materials [15, 16].

A good fuel cladding material has to satisfy a few selection criteria, which includes resistance to radiation, ability to withstand high service temperature and has a good fuel economy. During the fission reaction, radiation is produced while the temperature remains below 40% of the material's temperature, which further causes dislocation of loops resulting in the change of mechanical properties [19]. Lastly, the material has to be economic in terms of longevity and efficiency, this means that the material has to be resistant to corrosion and oxidation from other materials (coolant, moderator & fission products) in the reactor, the material also has to maintain a consistent thermal conductivity under high temperature as well as low thermal expansion to minimize damages to the cladding interface [13, 19, 20].

Beryllium (Be) was selected as an applicant for nuclear fuel cladding material owing to its exclusive characteristics (see Fig. 2 and Table 2). Besides that, be also exhibit an extreme corrosion behaviour when the service temperature exceeds 500°C, rendering the material unusable in high thermal condition. Most researches nowadays concentrating on this material (Be) is mainly in the region of fusion reactors, the safety of the material and its radiation resistance still poses great challenge for its successful application [23-27].

Representation of plutonium reactor in Hanford using Al fuel cladding is shown in Fig. 3. Even though Aluminium has a good corrosion resistance with low neutron absorption cross section, it has a maximum temperature at 200°C and this is considered insufficient for use in initial nuclear reactors. Therefore, Al was substituted by austenitic stainless steel by the United States [26, 28-31].

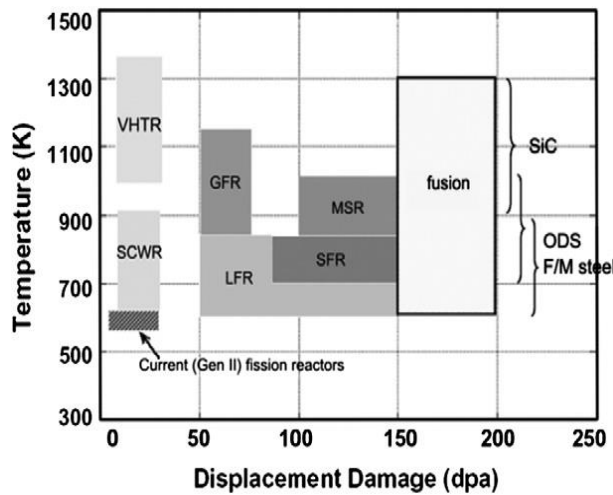
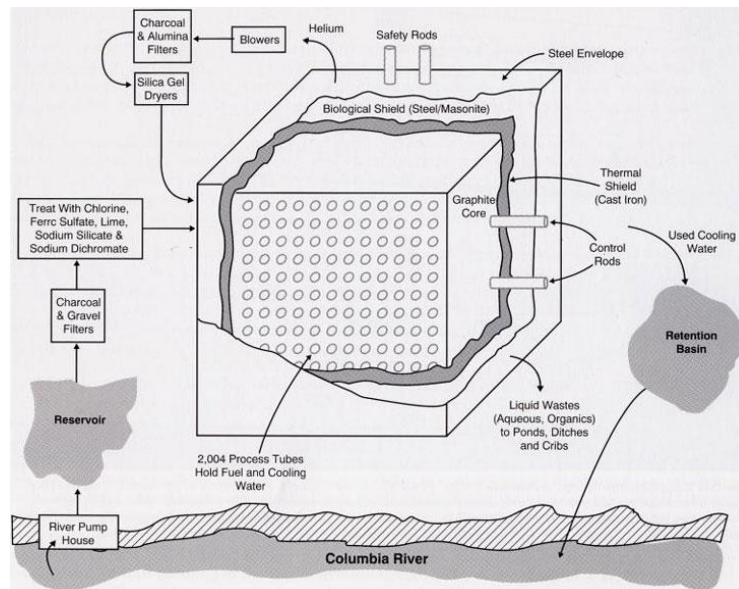


Fig. 2. GII and GIV design constraints [34].

**Table 2. Calculated effective neutron absorption cross section for pure elements in comparison to Zr [13, 16-18].**

Elements	Neutron absorption cross section (Barns)	Yield strength (MPa)	Relative effective neutron absorption cross section in relation to Zr
Be	0.009	200-350	0.04
C	0.004	24-28	0.2
Mg	0.063	65-100	1
Si	0.160	165-180	1
Zr	0.185	135-310	1
Al	0.231	30-40	8
Mo	2.480	170-350	10
Cr	3.050	185-280	15
Nb	1.150	75-95	15
Fe	2.550	110-165	20
Ni	4.430	80-280	30
V	5.040	125-180	40
Sn	0.630	7-15	70



**Fig. 3. Representation of plutonium reactor in Hanford using Al fuel cladding.**

In the 1960s, France, the UNGG design was replaced by the pressurized water reactor (PWR) while the Magnox reactor was further refined to advanced gas-cooled reactor (AGR) [18, 26].

AGR reactor allowed greater thermal efficiency than GCR reactor because the usage of austenitic stainless steel [18]. At low irradiation temperatures, fast neutrons instigates loss of ductility, while at higher temperatures Helium(He)formed by thermal neutron ( $\eta$ ,  $\alpha$ ) reactions stimulates low ductility due to gas-induced intergranular cracking [32, 33].

### 3. Current Trend Of Cladding Material

Several materials, such as ferritic-martensitic stainless steel (F/M steel), oxide dispersion increased (ODS) alloy, nickel-based super alloys, refractory metals and ceramic materials have already been suggested as applicant fuel cladding materials for GIV reactors, (see Table 3.) [34-45].

**Table 3. Main features of GIV nuclear fission reactor system [35-43].**

Reactor type	Fuel	Coolant	Moderator	Neutron spectrum	Core outlet temperature (°C)	Dose (dpa)	Candidate cladding material
<b>Super critical water-cooled reactor (SCWR)</b>	UO <sub>2</sub>	Water		Thermal	550	10-40	Zr alloys
	(thermal)			or			Austenitic stainless steel
	MOX	(fast)		Fast	F/M steel		
	(fast)			Ni-based superalloys			
						ODS alloys	
<b>Sodium-cooled fast reactor (SFR)</b>	UPuC/SiC U-Pu-Zr MOX	Liquid Na	-	Fast	550	90-160	F/M steels ODS alloys
<b>Lead-cooled reactor (LFR)</b>	Nitrides, MOX	Liquid Pb alloys	-	Fast	550-800	50-130	Austenitic stainless steel F/M steels ODS alloys SiC Refractory alloys
<b>Gas-cooled fast reactor (GFR)</b>	(U, Pu)O <sub>2</sub> Carbide fuel (U, Pu)	He	-	Fast	850	50-90	ODS alloys Refractory alloys SiC
<b>Molten salt reactor (MSR)</b>	Salt	Molten salt	Graphite	Thermal	700-800	100-180	No cladding
<b>Very high temperature reactor (VHTR)</b>	TRISO UOC	He	Graphite (thermal)	Thermal or fast	1000	7-30	ZrC coating SiC coating

The major hindrance for the selection of cladding materials and the viability of some of the GIV reactors are high temperature, high fast neutron radiation dose, violent environment and longer in-service life (see Table 3.) [35-43].

These flaws might generate changes in the mechanical, corrosion and physical properties of the cladding material [19, 34, 35, 46-48].

### 3.1. Zirconium Alloys

The shielding functioning of the oxide layer has been associated with the texture of the oxide microstructure and the existence of interfacial tetragonal  $Zr_3O$  along with monoclinic  $Zr_2O$ , but the use of Zr alloys as cladding material still limits the temperature to less than 400 °C [17, 37, 49, 50]. Hence, struggles are certainly desirable to increase the high temperature corrosion resistance of Zr alloys, though the understanding of the corrosion mechanism and the role of alloying elements and microstructure are still indeterminate [51-57].

### 3.2. Stainless Steels

Radiation damage, like huge amount of void swelling, radiation-induced segregation and microstructural unpredictability, remains a key performance-limiting feature in austenitic stainless steel [32, 33, 37]. These encompass doping with trace elements, cold deformation and precipitation of dispersed phases, in order to evade void swelling [58-60]. Ferritic and martensitic (F/M) stainless steels that displaying 9-12% of Cr, are probable applicants for the cladding material in a few GIV reactors [61-66].

### 3.3. Ceramic Materials - SiC

The main complications of GFR reactor's cladding are high fast-neutron impairment resistant and high temperature contact. Instead, there is an apprehension about the chemical compatibility of the cladding material with the Pb or Pb-Bi coolant and the mixed nitride fuel in LFR reactors.

SiC and SiC/SiC are being taken as the key candidate materials for GFR, LFR and VHTR reactor's fuel cladding. SiC composites have presented worthy irradiation performance and ability of mechanical properties at radiation damage levels beyond 50 dpa at temperatures around 1000°C [67, 68, 71].

### 3.4. Ni Based alloy

Ni alloys as a cladding material, with enhanced microstructural properties and radiation-resistant BCC matrix, are more favorable to avoid the radiation harmful effects [37, 38, 42, 66, 72, 73].

### 3.5. Refractory alloy

Applicant materials for fuel cladding of LFR and GFR reactors are refractory metal, with temperatures (see Table 3. and Fig. 4) [35, 37]. Furthermost of them are not candidate materials for fuel cladding due to their excessive values of neutron absorption cross section (see Fig. 5 and Table 4.).

### 3.6. ODS alloys

A significant method for designing the microstructure of this alloys is formed on the outline of a high, irradiation-stable nanoscale particles and uniform density of thermal, using particles of Titania ( $TiO_2$ ) and Yttria ( $Y_2O_3$ ) dispersed in a tempered or ferritic martensitic matrix, with chemical composition standard of F/M stainless steels or Fe-Cr Incoloy [35, 74]. These Nano-particles are thought to act promptly as sinks for the radiation-induced point defects,

bringing good radiation damage resistance and obstacles to dislocation motion [35, 37, 38,74-77].

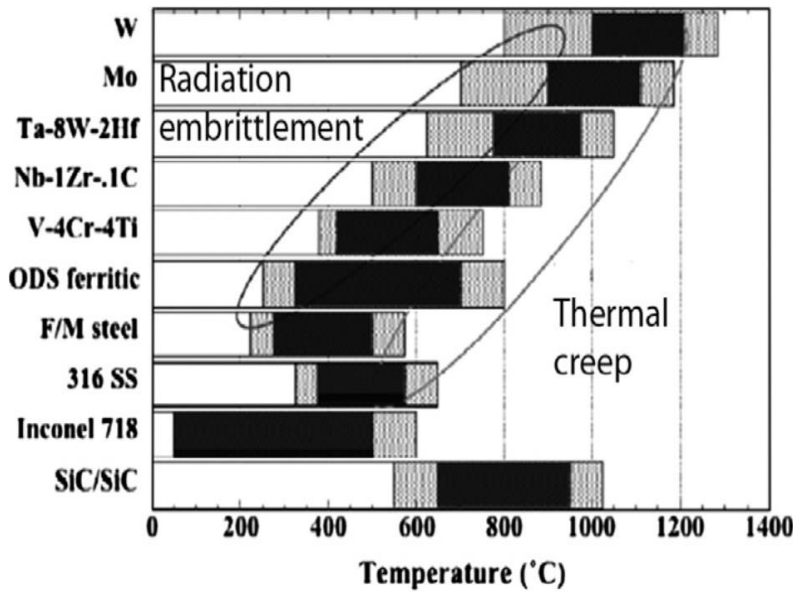


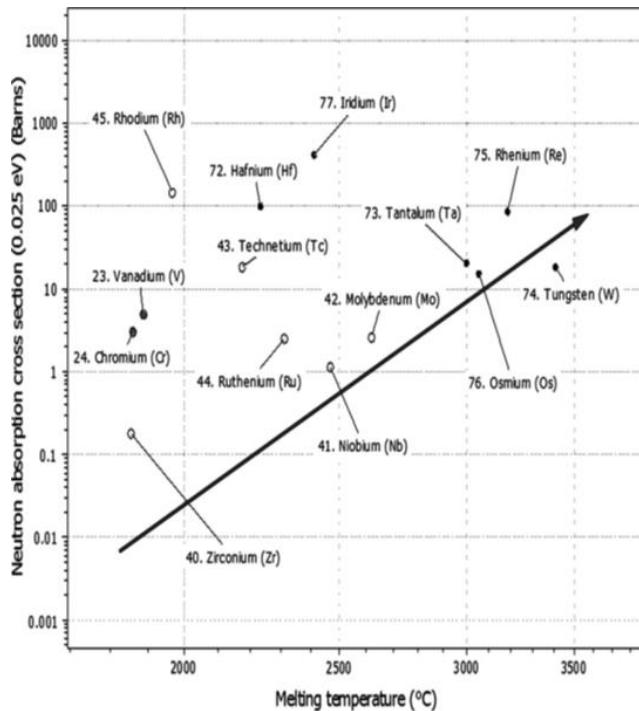
Fig. 4. Projected functioning temperature window for structural materials [35].

Table 4. Operative neutron absorption cross section and extreme service temperature for designated materials [18, 35].

Material	Maximum service Temperature=(°C)	Operative neutron absorption cross section in relation to Zr alloys
ODS alloys	700	15
Nb-1Zr alloy	800	20
ZrC	900	0.20
SiC	900	0.10
Tantalum alloys	1000	50
Molybdenum alloys	1100	10
Tungsten alloys	1200	35

Based on neutron irradiation





**Fig. 5. Neutron absorption cross section versus melting temperature for pure elements [18].**

#### 4. Cladding Failure In PWR

Fuel failure happens when this barrier is damaged and broken. It adds to cumulative plant background radiation, which impacts planned outages and increases workers' exposure. It can also pay to the issue of radioactive fission products to the environment [21].

##### 4.1. Loss of coolant

Loss of coolant (LOCA) happens when supplies tubes external to the reactor are damaged, that instigated the preventing the coolant attainment the first wall or plasma facing the components [78]. This may lead to the creation of steam in the core. Large amount of hydrogen gas was released when zirconium and high temperature steam interacted [79, 80]. The uncontrolled condition may lead to the zirconium-based alloy to loss its integrity [14, 81]. A hot spot of thermal limits was encounter when a large break was encounter. The thermal limits were encounter before the accumulator was activated [82]. Initial conditions for hot and intermediate shutdown LOCA are mentioned in Table 5.

Ballooning performance is a vital factor affecting the reliability of the cladding. Ballooning and rupture process of nuclear fuel cladding typically happens during actual LOCA events in pressurized water reactors (PWR) [83]. This may outcome in a coolant channel obstruction in the fuel assembly and stern loss of cool able geometry [84]. Temperature and interior pressure profiles for the Zr cladding specimens with and without a Cr coating layer during integral LOCA tests are

mentioned in Fig. 6. And photos of the ballooned areas and burst openings of Zr cladding specimens with and without Cr coating after essential LOCA and mechanical testing. Mentioned in Fig. 7. Optical microscopy imageries of cross sections at the burst mid-planes of a Cr-coated and uncoated Zr cladding tube, respectively. Optical microscopy imageries of the cross-sections 180 from the burst opening of a Cr-coated and uncoated Zr cladding tube, respectively.

**4.2. Corrosion**

The fuel rods can be corrosive when submerged in the primary water [86]. The corrosion reaction of zirconium metal in water will generate an oxide layer and the generation of hydrogen shown in Eq. (1) [87, 88]. The process is called oxidation process.



Relocation of the oxide by hopping mechanism when new oxide releases electrons to decrease the hydrogen ions at the cathodic site [89]. Several hydrogen will not be recombining with electrons at the oxide or water interface but are instead absorbed by the oxide layer and thus, metal is formed. This occurrence is called hydrogen pickup [90]. The corrosion process in Zirconium alloys is mentioned in Fig. 8.

**Table 5. Initial conditions for hot and intermediate shutdown LOCA [80].**

Parameter	Hot	Intermediate
Primary System(hot leg) Pressure /temperature (bar/K)	70.5/5203	70.5/450.1
Sub cooling margin, $\Delta T_{sub}$ (K)	39.2	100.7
Primary System (cold leg) temperature (K)	520.0	449.7
Secondary System pressure/temperature (bar/K)	37.0/518.9	9.1/449.2
Primary loop flow (combined) (kg/K)	6616	6925
Decay heat level (MW)	10.36 (0.917%)	9.77(0.865%)

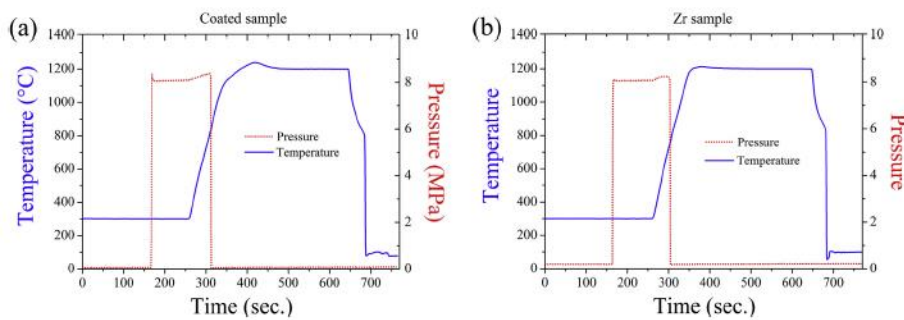


**Fig. 6. Temperature and interior pressure profiles for the Zr cladding specimens (a) with and (b) without a Cr coating layer during integral LOCA tests [86].**

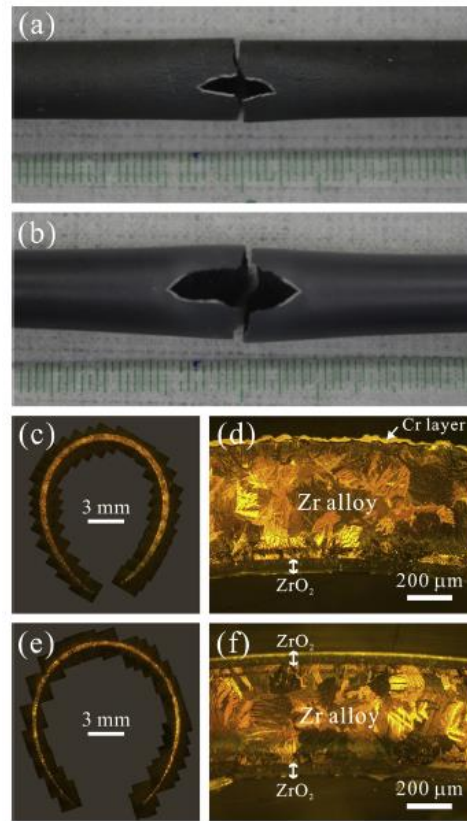


**Fig. 7. Photos of the ballooned areas and burst openings of Zr cladding specimens (a) with and (b) without Cr coating after essential LOCA and mechanical testing. (c, e) Optical microscopy imageries of cross sections at the burst mid-planes of a Cr-coated and uncoated Zr cladding tube, respectively. (d, f) Optical microscopy imageries of the cross-sections 180 from the burst opening of a Cr-coated and uncoated Zr cladding tube, respectively[85].**

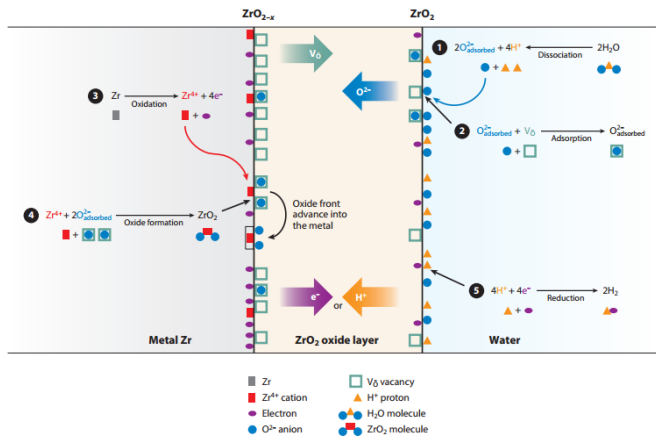


**Fig. 8. The corrosion process in Zirconium alloys [88].**

### 4.3. Creep

Creep is a time dependent deformation due to applied load [91]. It can be produced in two ways, which are by thermal or irradiation. The thermal creep consists of 3 stages as shown in Fig. 9. At the primary stage, the thermal creep is in initial rapid and slows with time. Then, the thermal creep will eventually shows a uniform rate in secondary stage and finally, the thermal creep will be in accelerated rate, which leads to rupture. The cladding of Zircaloy will show different behavior at range of temperature of 550-650°C at different stresses. Kuttayet al. [92] proposed the typical impression of creep curves for the alloy at different temperatures for a particular stress of 22.2MPa as shown in Fig. 10. The creep starts to show when the temperature at 575°C where the creep curves is not smooth. This is due to various stages of creep curve at all the stresses correspond to that temperature, as referred in Fig. 10 [93].

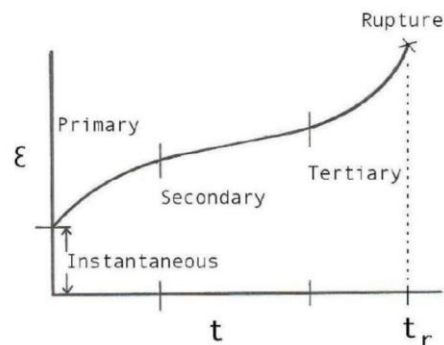


Fig. 9. Creep stages.

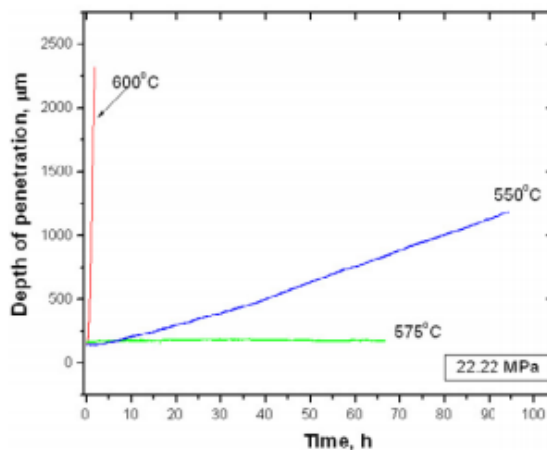
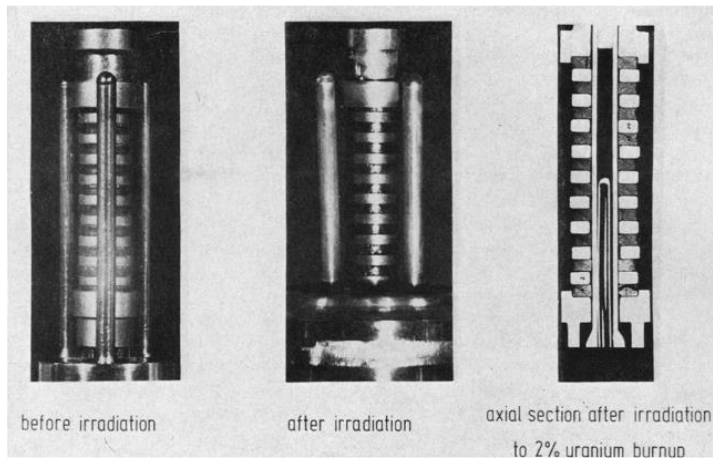


Fig. 10. The impression of creep curves for the alloy at different temperatures for a stress of 22.2 MPa are referred in Fig. 10 [93].

Irradiation creep do occur due to radiation released by fission process of the fuel. Figure 11 shows a creep when irradiated stack of annular UO<sub>2</sub> pellets and molybdenum rings. This is because point defects generated is at the heart of the irradiation creep process. In irradiation creep, it can be categorized into two types,

which are radiation-induced creep and radiation-enhanced creep. Radiation-induced creep occurs at lower temperatures at which thermal creep is not thermally activated. At this point, the creep is independent with temperature. When at lower temperature regions, production of vacancy concentration by atomic displacements because of irradiation will be large enough to induce creep deformation under the application of stress. Radiation-enhanced creep on the other hand is the process of creep which enhanced by irradiation. At homogeneous temperatures, the radiation-enhanced creep as well as thermal creep is operated. The vacancies increase when higher temperature applied. This can be translated into the increase of diffusivity. The addition of more vacancies can produce through fast neutron irradiation can enhancing the overall creep rate.



**Fig. 11. Creep when irradiated stack of annular UO<sub>2</sub> pellets and molybdenum rings [93].**

#### 4.4. Pellet cladding mechanical interaction (PCMI)

Pellet cladding mechanical interaction catastrophes will be initiated during fuel power changes are combined at locations where there are flaws in the fuel pellet exteriors [94]. They incline to propagate towards the centre of the pellet. It can be shown through analysis of the stresses that the resultant pellet wedges will relocate radially outward [95]. Stress concentrations between the edges of these wedges are complimentary points for cladding crack initiation [96].

#### 4.5. Denature from nucleate boiling

During the film boiling process, the heat transfer coefficient decreases expressively, resulting in prompt increases in clad and fuel temperatures [97]. This condition is devoted to as the departure of nucleate boiling ratio and is defined as:

$$DNBR = \frac{q'_{crit}}{q'} \quad (2)$$

Higher the unity ratio, higher the reactor safety margin during operation. For a particular fluid and experimental configuration, it is pre-determined what heat flux would result in the departure of nucleate boiling. Fuel temperature and pool temperature as a function of time of operation at 1 MW during one day in July of

2011 is shown in Fig. 12 and Comparison of fuel temperature computed with Dittus-Boelter and natural convection correlations as a function of pool temperature is shown in Fig. 13.

The operation of film boiling will result in high cladding temperature within the film boiling zone [99]. The chemical reactions, which occur between the two materials, become significant at temperature above 1100K. Fuel temperature within the film boiling zone rise rapidly due to DNB.

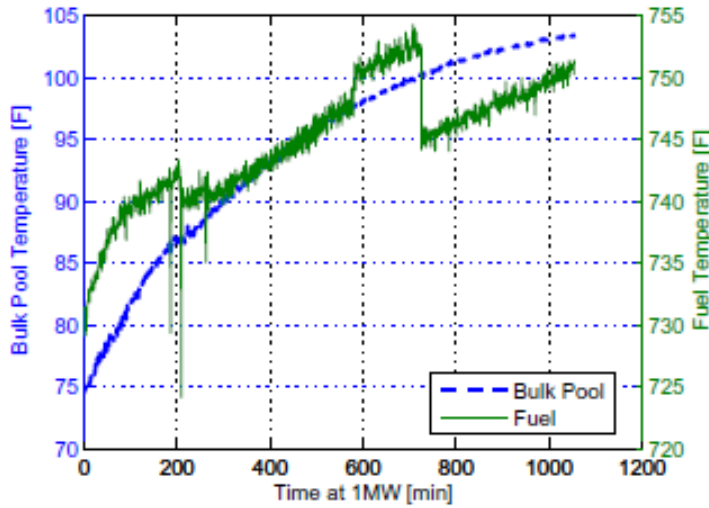


Fig. 12. Fuel temperature and pool temperature as a function of time of operation at 1 MW during one day in July of 2011 [99].

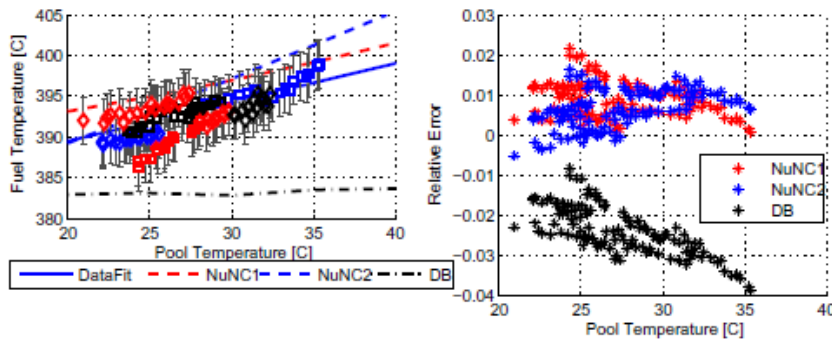


Fig. 13. Comparison of fuel temperature computed with Dittus-Boelter and natural convection correlations as a function of pool temperature [98].

The fuel temperature being above the equicohesive temperature of about 1900 K, at which grain boundary strength is less than the grain strength in UO<sub>2</sub> [100]. Fuel rod swelling has been observed in the film boiling zones of both previously unirradiated and, as shown in Figure 14, previously irradiated fuel rods. Only about half of the swelling is due to pellet thermal expansion and pellet volume expansion due to fuel melting. The remaining expansion is attributed primarily to fission gas

effects [101]. Post-test diametric measurements showing diameter increase in the film boiling zone of an earlier irradiated fuel rod are referred in Fig. 15.

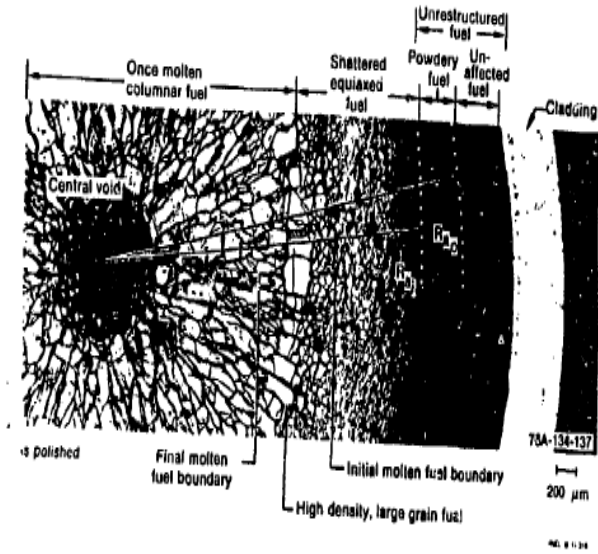


Fig. 14. Grain boundary separation has been observed in fuel from the film boiling [100].

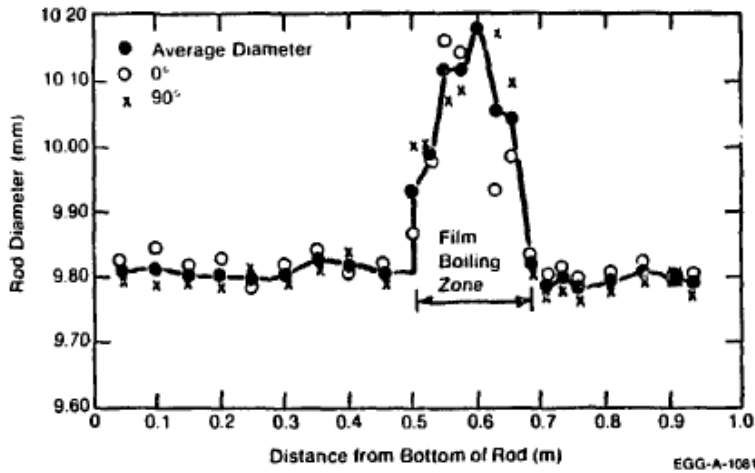


Fig. 15. Post-test diametric measurements showing diameter increase in the film boiling zone of an earlier irradiated fuel rod, Rod IE-010, Test IE-1 [100].

### 5. Conclusion

The integrity of cladding tube is very important as it contribute to release of radioactive fission product to the environment. Hence, it is also crucial to investigate the cladding failures so that effective measures can be taken to minimize the impact.

Several cladding failures in the current commercial nuclear power plant have been discussed. Increase in corrosion and creep rate during LOCA are significant. During corrosion, oxide layers formed on the clad surface are brittle which would endanger the structural integrity. Creep deformation cause cladding tube ballooning. The pellet radial cracking will occur due to PCMI. Lastly, DNB which resulting in rapid increases in cladding temperatures will reduce the reactor safety margin.

### Acknowledgment

This work is supported by the Ministry of Higher Education (MOE) Malaysia through Fundamental Research Grant No. FRGS/1/2016/TK03/UNITEN/02/1 and FRGS-UTM4F420.

### References

1. Director General of International Atomic Energy Agency. (2015). The Fukushima Daiichi accident report. Retrieved June 5, 2018, from <https://www-pub.iaea.org/books/IAEABooks/10962/The-Fukushima-Daiichi-Accident>.
2. Tokyo Electric Power Company (TEPCO). (2012). Fukushima Nuclear Accident Analysis Report. Retrieved June 5, 2018, from [http://www.tepco.co.jp/en/press/corp-com/release/betu12\\_e/images/120620e0102.pdf](http://www.tepco.co.jp/en/press/corp-com/release/betu12_e/images/120620e0102.pdf).
3. Hayashi, M.; and Hughes, L. (2013). The policy responses to the Fukushima nuclear accident and their effect on Japanese energy security. *Energy Policy*, 59, 86-101.
4. Feinroth, H.; Ales, M.; Barringer, E.; Kohse, G.; Carpenter, D.; and Jaramillo, R. (2010). Mechanical Strength of CTP TRIPLEX Clad Tubes After Irradiation in MIT Research Reactor Under PWR Coolant Conditions. *Ceramics in Nuclear Applications*, 47-55.
5. Katoh, Y. (2007). Current status and critical issues for development of SiC composites for fusion applications. *Journal of Nuclear Materials*, 367-370 A(SPEC. ISS.), 659-671.
6. Carmack, J.; Goldner, F.; Bragg-Sitton, S.M.; and Snead, L.L. (2013). Overview of the U.S. DOE Accident Tolerant Fuel Development Program. United States: Retrieved June 5, 2018, from <https://www.osti.gov/biblio/1130553>.
7. E. Research. (2012). Types of Nuclear Reactor. Retrieved June 5, 2018, from <https://ieer.org/resource/classroom/types-of-nuclear-reactors/>.
8. Kula, E. (2015). Future generations and nuclear power-A pluralistic economic appraisal. *Futures*, 73, 37-47.
9. Lamarsh, J.R.; and Baratta, A.J. (1955). *Introduction to Nuclear Engineering* (3rd ed.). New Jersey: Publisher, Prentice hall.
10. Rouben, B. (2001). CANDU Fuel-Management Course. *CANDU Fuel Management Course*. Ben Rouben, AECL. Retrieved June 5, 2018, from <https://canteach.candu.org/Content Library/20031101.pdf>.
11. Organisation for Economic Co-operation and Development (OECD). (1998). Shielding Aspects of Accelerators, Targets and Irradiation Facilities – SATIF



4. Retrieved June 7, 2018, from <https://www.oecd-nea.org/science/pubs/1999/1468-SATIF-4.pdf>.
12. Nonbel, E. (1996). *Description of the Advanced Gas Cooled Type of Gas Cooled Reactor*. Roskilde, Denmark, Riso National Laboratory.
  13. Wikmark, G.; Hallstadius, L.; and Yueh, K. (2009). Cladding to sustain corrosion, creep and growth at high burn-ups. *Nuclear Engineering and Technology*, 14(2), 143-148.
  14. Zinkle, S.J.; and Was, G.S. (2013). Materials challenges in nuclear energy. *Acta Materialia*, 61(3), 735-758.
  15. Kumar, G. (2016). Burst Ductility of Zirconium Clads: The Defining Role of Residual Stress. *Metallurgical and Materials Transactions A: Physical Metallurgy and Materials Science*, 47(8), 3882-3896.
  16. Northwood, D.O. (1985). The development and applications of zirconium alloys. *Materials & Design*, 6(2), 58-70.
  17. Motta, A.T. et al. (2007). Zirconium alloys for supercritical water reactor applications: Challenges and possibilities. *Journal of Nuclear Materials*, 371(1-3), 61-75.
  18. Griffin, R.B. (2004). Use of cambridge engineering selector in a materials/manufacturing course. *ASEE Annual Conference Proceedings*, 14723-14730.
  19. Azevedo, C.R.F. (2011). A review on neutron-irradiation-induced hardening of metallic components. *Engineering Failure Analysis*, 18(8), 1921-1942.
  20. Sullivan, M.A.; Stenger, D.; Roma, A.; and Tynan, M. (2014). The Future of Nuclear Power. *The Electricity Journal*, 27(4), 7-15.
  21. International Energy Atomic Agency (IAEA). (2010). Review of Fuel Failures in Water Cooled Reactors. *IAEA Nuclear Energy Series*, NF-T-2.1, 1-171.
  22. Alam, T.; Khan, M.K.; Pathak, M.; Ravi, K.; Singh, R.; Gupta, S.K. (2011). A review on the clad failure studies. *Nuclear Engineering and Design*, 241, 3658-3677.
  23. Ells, C.E.; and Perryman, E.C.W. (1959). Effects of neutron-induced gas formation on beryllium. *Journal of Nuclear Materials*, 1(1), 73-84.
  24. Raine, T.; and Robinson, J.A. (1962). The development and properties of beryllium-calcium alloys for use in high temperature, high pressure carbon dioxide. *Journal of Nuclear Materials*, 7(3), 263-278.
  25. McCoy Jr., H.E. (1965). Oxidation of beryllium in {CO<sub>2</sub>} by autoradiographic techniques. *Journal of Nuclear Materials*, 15(4), 249-262.
  26. Wanklyn, J.N.; and Jones, P.J. (1962). The aqueous corrosion of reactor metals. *Journal of Nuclear Materials*, 6(3), 291-329.
  27. Snead, L.L.; and Zinkle, S.J. (2005). Use of beryllium and beryllium oxide in space reactors. in *AIP Conference Proceedings*, 746, 768-775.
  28. Ronen, Y.; and Raitzes, G. (2004). Ultra-thin <sup>242m</sup>Am fuel elements in nuclear reactors. II. *Nuclear Instruments Methods in Physics Research Section A: Acceleration, Spectrometers, Detectors and Associated Equipment*, 522(3), 558-567.
  29. Nightingale, R.E. (1962). *Nuclear Graphite*. New York: Acadamec Press.

30. Kim, Y.S.; Hofman, G.L.; Robinson, A.B.; Snelgrove, J.L.; and Hanan, N.(2008). Oxidation of Aluminum alloy cladding for research and test reactor fuel. *Journal of Nuclear Materials*, 378(2), 220-228.
31. Leenaers, A.; Detavernier, C.; and Van den Berghe, S. (2008). The effect of silicon on the interaction between metallic Uranium and Aluminum: A 50 year long diffusion experiment. *Journal of Nuclear Materials*, 381(3), 242-248.
32. Klueh, R.L.; and Vitek, J.M. (1985). Elevated-temperature tensile properties of irradiated 9 Cr-1 MoVNb steel. *Journal of Nuclear Materials*, 132(1), 27-31.
33. Walker, S.P.; Yu, A.; and Fenner, R.T. (1992). Pellet-clad mechanical interaction: pellet-clad bond failure and strain relief. *Nuclear Engineering and Design*, 138(3), 403-408.
34. Little, E.A. (2006). Development of radiation resistant materials for advanced nuclear power plant. *Materials Science and Technology*, 22(5), 491-518.
35. Zinkle, S.J.; and Busby, J.T. (2009). Structural materials for fission & fusion energy. *Materials Today*, 12(11), 12-19.
36. Azevedo, C.R.F. (2011). Selection of fuel cladding material for nuclear fission reactors. *Engineering Failure Analysis*, 18(8), 1943-1962.
37. Murty, K.L.; and Charit, I. (2008). Structural materials for Gen-IV nuclear reactors: Challenges and opportunities. *Journal of Nuclear Materials*, 383(1-2), 189-195.
38. Raj, B.; Mannan, S.L.; Rao, P.R.V.; and Mathew, M.D.(2002). Development of fuels and structural materials for fast breeder reactors. *Sadhana*, 27(5), 527-558.
39. DoE, U. (2002). A technology roadmap for generation IV nuclear energy systems. *Nuclear Energy Research Advisory Committee*, 1-97.
40. Yvon, P.; and Carré, F.(2009). Structural materials challenges for advanced reactor systems. *Journal of Nuclear Materials*, 385(2), 217-222.
41. Abram, T.; and Ion, S. (2008). Generation-IV nuclear power: A review of the state of the science. *Energy Policy*, 36(12), 4323-4330.
42. Fazio, C.*et al.* (2009). European cross-cutting research on structural materials for Generation IV and transmutation systems. *Journal of Nuclear Materials*, 392(2), 316-323.
43. Bohr, N.; and Wheeler, J.A. (1939). The mechanism of nuclear fission. *Physical Review*, 56(5), 426-450.
44. Baindur, S. (2008). Materials challenges for the supercritical water cooled reactor (SCWR). *Bulletin of the Canadian Nuclear Society*, 29(1), 32-38.
45. Ehrlich, K.; Konys, J.; and Heikinheimo, L. (2004). Materials for high performance light water reactors. *Journal of Nuclear Materials*, 327(2-3), 140-147.
46. Squarer, D. (2003). High performance light water reactor. *Nuclear Engineering and Design*, 221(1-3) SPEC., 167-180.
47. Mansur, L.K.; Rowcliffe, A.F.; Nanstad, R.K.; Zinkle, S.J.; Corwin, W.R.; and Stoller, R.E. (2004). Materials needs for fusion, Generation IV fission reactors and spallation neutron sources - Similarities and differences. *Journal of Nuclear Materials*, 329-333 (1-3 PART A), 166-172.
48. Motta, A.T. (2008). Microstructural Characterization of Oxides Formed on Model Zr Alloys Using Synchrotron Radiation. *Journal of ASTM International*, 5(3), 1-20.

49. Le Saux, M.; Besson, J.; Carassou, S.; Poussard, C.; and Averty, X. (2010). Behavior and failure of uniformly hydrided Zircaloy-4 fuel claddings between 25 °C and 480 °C under various stress states, including RIA loading conditions. *Engineering Failure Analysis*, 17(3), 683-700.
50. Cox, B. (2005). Some thoughts on the mechanisms of in-reactor corrosion of Zirconium Alloys. *Journal of Nuclear Materials*, 336(2-3), 331-368.
51. Cox, B.; Pemsler, J.P.; and Bchantillons, D. (1968). Diffusion of oxygen in growing Zirconia films. *Journal of Nuclear Materials*, 28, 73-78.
52. Cox, B. (1968). Effects of irradiation on the oxidation of zirconium alloys in high temperature aqueous environments: A review. *Journal of Nuclear Materials*, 28(1), 1-47.
53. Bossis, P.; Pêcheur, D.; Hanifi, K.; Thomazet, J.; Blat, M.; and Yagnik, S. (2005). Comparison of the high burn-up corrosion on M5 and low tin zircaloy-4. *ASTM Special Technical Publication*, 3(1467), 494-525.
54. Sabol, G.P. (2005). ZIRLO - An Alloy Development Success. *Journal of ASTM International*, 2(2), pp. 3-24.
55. Dupin, N.; Ansara, I.; Servant, C.; Toffolon, C.; Lemaignan, C.; and Brachet, J.C. (1999). Thermodynamic database for zirconium alloys. *Journal of Nuclear Materials*, 275(3), 287-295.
56. Krishnan, R.; and Asundi, M.K. (1981). Zirconium alloys in nuclear technology. *Proceedings of the Indian Academy Science Section C: Engineering Sciences*, 4(1), 41-56. doi: 10.1007/BF02843474.
57. Reiss, T.; Csom, G.; Fehér, S.; and Czifrus, S. (2010). The Simplified Supercritical Water-Cooled Reactor (SSCWR), a new SCWR design. *Progress in Nuclear Energy*, 52(2), 177-189.
58. Johnston, W.G.; Rosolowski, J.H.; Turkalo, A.M.; and Lauritzen, T. (1973). Nickel-ion bombardment of annealed and cold-worked type 316 stainless steel. *Journal of Nuclear Materials*, 48(3), 330-338.
59. Kurishita, H.; Kayano, H.; Narui, M.; Kimura, A.; Hamilton, M.L.; and Gelles, D.S. (1994). Tensile properties of reduced activation Fe-9Cr-2W steels after FFTF irradiation. *Journal of Nuclear Materials*, 212-215(PART 1), 730-735.
60. Sagaradze, V.V.; Lapin, S.S.; Kirk, M.A.; and Goshchitskii, B.N. (1999). Influence of high-dose Kr+ irradiation on structural evolution and swelling of 16Cr-15Ni-3Mo-1Ti aging steel. *Journal of Nuclear Materials*, 274(3), 287-298.
61. Klueh, R.L.; and Nelson, A.T. (2007). Ferritic/Martensitic steels for next-generation reactors. *Journal of Nuclear Materials*, 371(1-3), 37-52.
62. Lu, Z.; Faulkner, R.G.; and Flewitt, P.E.J. (2007). Irradiation-induced impurity segregation and ductile-to-brittle transition temperature shift in high Chromium Ferritic/Martensitic steels. *Journal of Nuclear Materials*, 367-370 A(SPEC. ISS.), 621-626.
63. Lu, Z.; Faulkner, R.G.; and Morgan, T.S. (2008). Formation of austenite in high Cr Ferritic/Martensitic steels by high fluence neutron irradiation. *Journal of Nuclear Materials*, 382(2-3), 223-228.
64. Kurtz, R.J. et al. (2009). Recent progress toward development of reduced activation Ferritic/Martensitic steels for fusion structural applications. *Journal of Nuclear Materials*, 386-388(C), 411-417.

65. Yano, Y.*et al.* (2010). Mechanical properties and microstructural stability of 11Cr-Ferritic/Martensitic steel cladding under irradiation. *Journal of Nuclear Materials*, 398(1-3), 59-63.
66. Rowcliffe, A.F.; Mansur, L.K.; Hoelzer, D.T.; and Nanstad, R.K. (2009). Perspectives on radiation effects in nickel-base alloys for applications in advanced reactors. *Journal of Nuclear Materials*, 392(2), 341-352.
67. Carpenter, D. (2006). Comparison of Pellet-Cladding Mechanical Interaction for Zircaloy and Silicon Carbide Clad Fuel Rods in Pressurized Water Reactors. *Ocw.Edu.Ht*, 20.
68. Meyer, M.K.; Fielding, R.; and Gan, J. (2007). Fuel development for gas-cooled fast reactors. *Journal of Nuclear Materials*, 371(1-3), 281-287.
69. Ueta, S.; Aihara, J.; Yasuda, A.; Ishibashi, H.; Takayama, T.; and Sawa, K. (2008). Fabrication of uniform ZrC coating layer for the coated fuel particle of the very high temperature reactor. *Journal of Nuclear Materials*, 376(2), 146-151.
70. Yang, Y.; Dickerson, C.A.; Swoboda, H.; Miller, B.; and Allen, T.R. (2008). Microstructure and mechanical properties of proton irradiated zirconium carbide. *Journal of Nuclear Materials*, 378(3), 341-348.
71. Wongsawaeng, D. (2010). Performance modeling of Deep Burn TRISO fuel using ZrC as a load-bearing layer and an oxygen getter. *Journal of Nuclear Materials*, 396(2-3), 149-158.
72. Boothby, R.M. (1996). The microstructure of fast neutron irradiated nimonic PE16. *Journal of Nuclear Materials*, 230(2), 148-157.
73. Angeliu, T.M.; Ward, J.T.; and Witter, J.K. (2007) Assessing the effects of radiation damage on Ni-base alloys for the prometheus space reactor system. *Journal of Nuclear Materials*, 366(1-2), 223-237.
74. El-Genk, M.S.; and Tournier, J.M. (2005). A review of refractory metal alloys and mechanically alloyed-oxide dispersion strengthened steels for space nuclear power systems. *Journal of Nuclear Materials*, 340(1), 93-112.
75. Ukai, S.; and Fujiwara, M. (2002) Perspective of ODS alloys application in nuclear environments. *Journal of Nuclear Materials*, 307-311(1), 749-757.
76. Yoshida, E.; and Kato, S. (2004). Sodium compatibility of ODS steel at elevated temperature. *Journal of Nuclear Materials*, 329-333(1-3 PART B), 1393-1397.
77. Schroer, C.; Konys, J.; Furukawa, T.; and Aoto, K. (2010). Oxidation behaviour of P122 and a 9Cr-2W ODS steel at 550 °C in oxygen-containing flowing lead-bismuth eutectic. *Journal of Nuclear Materials*, 398(1-3), 109-115.
78. Mogahed, E.A.; El-Guebaly, L.; Abdou, A.; Wilson, P.; Henderson, D.; and Team, A. (2001). Loss of coolant accident and loss of flow accident analysis of the ARIES-AT design. *Fusion Technology*, 39(2), 462-466.
79. Kurata, M. (2016). Research and Development Methodology for Practical Use of Accident Tolerant Fuel in Light Water Reactors. *Nuclear Engineering and Technology*, 48(1), 26-32.
80. Nishimura, T.; Hoshi, H.; and Hotta, A. (2015). Current research and development activities on fission products and hydrogen risk after the accident at Fukushima Daiichi Nuclear Power Station. *Nuclear Engineering and Technology*, 47(1), 1-10.

81. Ott, L.J.; Robb, K.R.; and Wang, D. (2015). Preliminary assessment of accident-tolerant fuels on LWR performance during normal operation and under DB and BDB accident conditions. *Journal of Nuclear Materials*, 461, 178-179.
82. Bokhari, I.H.; and Mahmood, T. (2005). Analysis of loss of flow accident at Pakistan research reactor-1. *Annals of Nuclear Energy*, 32(18), 1963-1968.
83. Terrani, K.A.; Wang, D.; Ott, L.J.; and Montgomery, R.O. (2014). The effect of fuel thermal conductivity on the behavior of LWR cores during loss-of-coolant accidents. *Journal of Nuclear Materials*, 448(1-3), 512-519.
84. Massey, C.P.; Terrani, K.A.; Dryepontd, S.N.; and Pint, B.A. (2016). Cladding burst behavior of Fe-based alloys under LOCA. *Journal of Nuclear Materials*, 470, 128-138.
85. Park, D.J.; Kim, H.G.; Il Jung, Y.; Park, J.H.; Yang, J.H.; and Koo, Y.H. (2016). Behavior of an improved Zr fuel cladding with oxidation resistant coating under loss-of-coolant accident conditions. *Journal of Nuclear Materials*, 482, 75-82.
86. Anwyl, C.; Boxall, C.; Wilbraham, R.; Hambley, D.; and Padovani, C. (2016). Corrosion of AGR Fuel Pin Steel under Conditions Relevant to Permanent Disposal. *Atalante 2016 International Conference On Nuclear Chemistry For Sustainable Fuel Cycles*, 21, 247-254.
87. Motta, A.T.; Couet, A.; and Comstock, R.J. (2015). Corrosion of Zirconium Alloys Used for Nuclear Fuel Cladding. *Annual Review of Materials Research*, 45(1), 311-343.
88. Ma, X.; Toffolon-Masclat, C.; Guilbert, T.; Hamon, D.; and Brachet, J.C. (2008). Oxidation kinetics and oxygen diffusion in low-tin Zircaloy-4 up to 1523 K. *Journal of Nuclear Materials*, 377(2), 359-369.
89. Ramasubramanian, N. (1975). Localised electron transport in corroding zirconium alloys. *Journal of Nuclear Materials*, 55(2), 134-154.
90. Motta, A.T.; and Chen, L.Q. (2012). Hydride formation in zirconium alloys. *JOM*, 64(12), 1403-1408.
91. Matthews, J.R.; and Finnis, M.W. (1988). Irradiation creep models - an overview. *Journal of Nuclear Materials*, 159(C), 257-285.
92. Kutty, T.R.G.; Kaity, S.; and Kumar, A. (2013). Impression creep behaviour of U-6%Zr alloy: Role of microstructure. *Procedia Engineering*, 55, 561-565.
93. Brucklacher, D.; and Dienst, W. (1972). Creep behavior of ceramic nuclear fuels under neutron irradiation. *Journal of Nuclear Materials*, 42(3), 285-296.
94. Allen, T.; Busby, J.; Meyer, M.; and Petti, D. (2010). Materials challenges for nuclear systems. *Materials Today*, 13(12), 14-23.
95. Helfer, T.; Garcia, P.; Ricaud, J.M.; Plancq, D.; and Struzik, C. (2004). *Modelling The Effect Of Oxide Fuel Fracturing On The Mechanical Behaviour Of Fuel Rods. in Pellet-clad Interaction in Water Reactor Fuels*. Paris: Nuclear Energy Agency.
96. Guicheret-Retel, V.; Trivaudey, F.; Boubakar, M.L.; Masson, R.; and Thevenin, P. (2004). *Modelling 3-D Mechanical Phenomena In A 1-D Industrial Finite Element Code: Results And Perspectives. in Pellet-clad Interaction in Water Reactor Fuel*. Paris: Nuclear Energy Agency.

97. Collier, J.G.; and Thome, J.R. (1994). *Convective boiling and condensation*.(3rd Ed.), Oxford University Press.
98. Johns, J.; and Reece, W.D. (2015). Subchannel analysis of fuel temperature and departure of nucleate boiling of TRIGA Mark i. *Annals of Nuclear Energy*, 75, 331-339.
99. Li, M.; and Zinkle, S.J. (2007). Fracture mechanism maps in unirradiated and irradiated metals and alloys. *Journal of Nuclear Materials*, 361(2-3 SPEC. ISS.), 192-205.
100. Cronenberg, A.W.; and Yackle, T.R. (1979). Intergranular fracture of unrestructured UO<sub>2</sub> fuel, during film-boiling operation. *Journal of Nuclear Materials*, 84(1-2), 295-318.
101. Maeda, K.; Katsuyama, K.; and Asaga, T. (2005). Fission gas release in FBR MOX fuel irradiated to high burnup. *Journal of Nuclear Materials*, 346(2-3), 244-252.